Available online at www.sciencedirect.com
SCIENCE DIRECT®
Journal of Nuclear Materials 336 (2005) 90–96
journal of nuclear materials
www.elsevier.com/locate/jnucmat

Small-angle neutron scattering study on the effect of hydrogen in irradiated reactor pressure vessel steels

A. Ulbricht [a,*], J. Böhmert [a], M. Uhlemann [b], G. Müller [a]

[a] *Forschungszentrum Rossendorf e.V., Institut für Sicherheitsforschung, P.O. Box 510119, D-01314 Dresden, Germany*
[b] *Institut für Festkörper- und Werkstoffforschung Dresden, Postfach 270016, D-01171 Dresden, Germany*

Received 15 March 2004; accepted 11 September 2004

Abstract

Hydrogen uptake can enhance the neutron embrittlement of reactor pressure vessel (RPV) steels. This suggests that irradiation defects act as hydrogen traps. The evidence of hydrogen trapping was investigated using the small-angle neutron scattering (SANS) method on four RPV steels. The samples were examined in the unirradiated and irradiated states and both in the as-received condition and after hydrogen charging. Despite the low bulk content of hydrogen achieved after charging with low current densities, an enrichment of hydrogen in small microstructural defects could be identified. Preferential traps were microstructural defects in the size range of $\approx > 10$ nm in the unirradiated and irradiated samples. However, the results do not show any evidence for hydrogen trapping in irradiation defects.

1. Introduction

The low alloy Cr–Mo and Cr–Ni steels used for nuclear pressure vessel (RPV) are considered to be susceptible to hydrogen embrittlement. Hydrogen embrittlement susceptibility can be especially observed for the high-strength steels and is affected by microstructural heterogeneities or particles that act as hydrogen traps [1]. In RPV steels additional microstructural heterogeneities are produced during the reactor operation due to neutron exposition and yield an increase of strength and a shift of the ductile brittle transition temperature known as irradiation embrittlement. Thus, it is not inept to assume that both phenomena interact, perhaps even in a synergistic manner. This would have a paramount impact on the RPV integrity assessment, particularly as, on the one hand, the conventional embrittlement surveillance programme does not cover the hydrogen effects and, on the other hand, radiolysis and corrosion may result in the hydrogen uptake during the service.

The risk was investigated early and assessed to be uncritical. According to Brinkman and Beeston [2] there is only a total loss of the tensile ductility for irradiated steels if the strength is larger than 1200 MPa and the concentration of hydrogen is higher than 1 ppm. For steels of lower strength, hydrogen concentrations of $\geqslant$2.5–4 ppm yield a degradation of the mechanical properties both in the unirradiated and in the irradiated conditions [2–9]. Irradiation enhances the effect, especially if the irradiation temperature is low.

* Corresponding author. Tel.: +49 351 260 3155; fax: +49 351 260 2205.
E-mail address: a.ulbricht@fz-rossendorf.de (A. Ulbricht).

0022-3115/$ - see front matter © 2004 Elsevier B.V. All rights reserved.
doi:10.1016/j.jnucmat.2004.09.005

Such high hydrogen concentrations are not expected under typical LWR conditions. This is borne by the results of in situ experiments of Splichal et al. [10] and Anders et al. [11].

Nevertheless, in the last years more effort has again been devoted the influence of hydrogen on the mechanical behaviour under irradiation. Although the recent work mainly relates to martensitic low activation Cr steels [12,13] which are proposed as structural steels for fusion reactor components or to austenitic stainless steels, which are potentially endangered by irradiation assisted stress corrosion cracking [14,15], there are remarkable activities to investigate low-alloyed ferritic RPV steels under this aspect as well [16–19].

A very new point of view was presented by Pachur [20]. He analyzed the results of a comprehensive German irradiation programme and additionally investigated irradiated and subsequently cathodically hydrogen-charged specimens from different RPV steels. On this base, he postulated that the radiation defects are traps for hydrogen and, furthermore, that the interaction hydrogen–irradiation is responsible for the mechanism III of the neutron-induced effects on the mechanical properties. The mechanism III was described by Pachur in a former paper [21] and was considered to act within the characteristic range of the service temperature of LWRs.

A decoration or enrichment of the radiation defects with hydrogen atoms should be indicated by the small-angle neutron scattering (SANS) effects. SANS has proved to be an effective method to investigate nanoscale microstructural heterogeneities induced by neutron irradiation. Hydrogen has a negative nuclear scattering length which is clearly different from the average nuclear scattering length of the steel matrix [22]. Thus, hydrogen in the radiation defects should be evident by an increase of the nuclear scattering contrast. The usefulness of the SANS method to investigate the interaction of hydrogen and microstructure has already been shown for other materials, e.g. the hydrogen–dislocation interaction in palladium [23–25] or the characterization of hydrogen defects in aluminium [26,27].

The paper reports on the results of SANS measurements on irradiated and hydrogen-charged samples made from RPV steels of different types. For comparison unirradiated reference samples of the same material were also tested. Probably, these are the first experiments in order to reveal the interrelation between radiation defects and hydrogen using the SANS method.

2. Evidence of hydrogen in SANS experiments

The differential macroscopic SANS cross-section $d\Sigma(Q)/d\Omega$, which is calculated from the measured SANS intensity by correction of the influence of the experimental conditions, is given by [28]

$$\frac{d\Sigma}{d\Omega}\left(\vec{Q}\right) = \frac{1}{V_S}\left[\int_{V_S} \Delta\eta(\vec{r}) e^{-i\vec{Q}\vec{r}}\, d^3\vec{r}\right]^2. \quad (1)$$

The quantity $\Delta\eta(\vec{r})$ means the difference of the coherent scattering length (=product of the number density of atoms n and the scattering length b) on the place $\vec{r}$ relating to the average value of the matrix. $\vec{Q}$ is the scattering vector and V_S is the sample volume.

For a two-phase model, the SANS cross-section and, thus, the scattering intensity increases with increasing scattering contrast $(\Delta\eta)^2$,

$$(\Delta\eta)^2 = (n_p \cdot b_p - n_M \cdot b_M)^2. \quad (2)$$

The quantities $n_p \cdot b_p$ and $n_M \cdot b_M$ are the above-mentioned parameters for the scattering particles (=radiation defects) and matrix, respectively.

The SANS cross-section consists of a nuclear and a magnetic component. The nuclear component is caused by the neutron scattering with the nuclei. The characteristic parameter is the neutron scattering length. It does not show a regular course with the atomic number, it is isotope-specific and can even take on negative values. The last one is valid for hydrogen with $b^H_{nuc} = -0.374 \times 10^{-12}$ cm [22].

In irradiated RPV steels, the scattering length densities of the matrix and the scattering defects are positive and the scattering length density of the radiation defects is lower than that of the matrix. Thus, the enrichment of hydrogen in radiation defects due to trapping will lead to an increase of the nuclear component of the SANS cross-section. In contrast to that, the magnetic component will not change because the hydrogen atom has no magnetic moment that is sufficiently large in order to be effective. Both SANS components can be separated, if SANS is measured in a saturated magnetic field

$$\frac{d\Sigma}{d\Omega}(\alpha) = \left(\frac{d\Sigma}{d\Omega}\right)_{nuc} + \left(\frac{\Delta\Sigma}{\Delta\Omega}\right)_{mag}, \quad (3)$$

with $\left(\frac{d\Sigma}{d\Omega}\right)_{nuc} = \frac{d\Sigma}{d\Omega}(\alpha = 0)$ and

$$\left(\frac{d\Sigma}{d\Omega}\right)_{mag} = \frac{d\Sigma}{d\Omega}\left(\alpha = \frac{\pi}{2}\right) - \frac{d\Sigma}{d\Omega}(\alpha = 0).$$

The quantity α is the angle between the magnetic field and the incident neutron beam.

The hydrogen trapping on the radiation defects does not only increase the nuclear SANS cross-section but also reduces the ratio between the nuclear and the total SANS cross-section (A-ratio).

The lower detection limit for hydrogen trapped in the radiation effects can be roughly estimated as follows: assuming that a 5% difference in the SANS intensity

due to the hydrogen trapping is sufficiently evident, then the detection limit, is given by

$$\frac{n_H}{n_M} = \left(\sqrt{1.05} - 1\right) \frac{\left|(b_M)_{nuc} - (b_p)_{nuc}\right|}{\left|(b_H)_{nuc}\right|}. \quad (4)$$

The quantity n_H is the number density of hydrogen atoms in the scattering particles relating to the number density n_M of the atoms in the matrix. $(b_M)_{nuc}$, $(b_p)_{nuc}$ and $(b_H)_{nuc}$ are the nuclear scattering lengths of matrix, particles and hydrogen, respectively. The scattering length of the radiation defects is unknown but a realistic estimation should be $(b_p)_{nuc} = |0.5(b_M)_{nuc}|$. This leads to a detection limit of < 3 at.% hydrogen per radiation defects. Thus, a hydrogen content of 1 ppm (56 at-ppm) can be detected, if the hydrogen atoms are mainly trapped in the radiation defects and the volume fraction of the radiation defects is 0.2%.

3. Experimental details

The materials and the irradiation conditions are listed in Tables 1 and 2. The materials comprise both base metals (JRQ, JPA, KAB) and weld metal (R19). JRQ and JPA are materials from the IAEA-CRP programme, phase 3, the KAB material is a Russian RPV steel, which is characteristic for the first VVER 440 generation, and R19 represents a VVER 1000-type weld metal. KAB-7 and -8 are cut from adjacent thickness positions of a forging (140 mm thick) in ≈1/4 thickness position.

The irradiation was executed in the VVER 2-prototype reactor in Rheinsberg (Germany). KAB-8 was irradiated in the Rossendorf Research Reactor RFR. Apart from this material the other materials showed high-SANS effects after irradiation. The volume fractions of the irradiation defects calculated from the magnetic cross-section are also given in Table 2. For this calculation the volume fraction distribution function was determined using the indirect transformation method according to Glatter [29] and the irradiation defects were assumed to be non-ferromagnetic.

For more details on material, irradiation and microstructure in the as-irradiated state the reader is referred to [30]. Slices of 0.8 mm thickness cut from broken Charpy impact specimens were used for the SANS experiments. Each material was investigated in the unirradiated and irradiated conditions and without and after hydrogen charging. For JRQ the samples in the hydrogen-uncharged and charged states were identical, for JPA, KAB-7 and KAB-8 the samples were directly adjacent slices cut from the same specimens, and for R19 slices from different Charpy impact specimens were used.

The slices were cathodically charged in simulated RPV water 0.1 M boric acid/0.01 M KOH with current densities of 5 mA/cm^2 up to saturation at room temperature. The hydrogen content was determined by hot extraction with the hydrogen analyzer LECO-RH 402. The charging condition was moderate and adapted to the conditions expected in the power water reactor. The aim of the treatment was not to achieve a very high, hypercritical hydrogen concentration, but to establish realistic conditions. Therefore, the hydrogen contents after charging were low and amounted to 1.8–2.5 ppm depending on the type of steel. In the as-received condition the hydrogen

Table 1
Chemical composition of materials (mass.%, Fe balance)

Material code	Type	C	Mn	Si	Cr	Ni	Mo	V	S	P	Cu	Al
JRQ	ASTM 533 B cl. 1	0.19	1.41	0.25	0.13	0.84	0.50	0.008	0.004	0.019	0.14	0.02
JPA	ASTM 533 B cl. 1 mod.	0.18	1.47	0.27	0.15	0.82	0.54	0.01	0.002	0.018	0.33	
KAB-7 KAB-8	15Xh2MFA	0.14	0.55	0.24	2.60	0.24	0.62	0.27	0.013	0.011	0.22	0.015
R19	10KhGMFAA	0.09	1.14	0.38	1.66	1.71	0.63	0.01	0.010	0.012	0.04	0.010

Table 2
Irradiation conditions

Material code	Reactor	Fluence ($E > 0.5$ MeV) 10^{18} n/cm^2	Temp., °C	Δc[a] vol.%
JRQ	VVER-2, Rheinsberg	133	255	0.50
JPA	VVER-2, Rheinsberg	80	255	0.75
KAB-7	VVER-2, Rheinsberg	139	255	0.26
KAB-8	RFR Rossendorf	27	> 60	0.07
R19	VVER-2, Rheinsberg	65	255	0.25

[a] Volume fraction of radiation defects.

concentrations were between 0.4 to 0.8 ppm. It was assumed, that only hydrogen in the solid solution effuses, whereas the stronger bonded hydrogen remains in the sample. Nevertheless, it was taken care to have a short time between hydrogen charging and the SANS experiments. During this time the samples were stored at low temperatures (dry ice, −78 °C).

The SANS experiments were executed on the spectrometer V4 of HMI Berlin [31]. The samples were placed in a saturating magnetic field of 1.3 T perpendicular to the neutron beam direction (wavelength = 0.6 nm, beam diameter = 7.5 mm). Two distances between sample and the two-dimensional 64-by-64-cm position-sensitive detector were used, covering a range of the scattering vector of 0.1–3.0 nm^{-1}. All data were corrected for background, transmission, and detector efficiency, and calibrated with a water standard using the HMI software routines [32].

The measured SANS cross-section curves always included a constant, Q-invariable scattering contribution. This incoherent contribution is caused by the different isotopes of the elements and the monotonous Laue scattering. It mainly contributes to the nuclear SANS component, it is larger than the pure isotope effect, and it is enhanced by irradiation. For further analysis the incoherent contribution was determined using the Porod approximation as described in [33]. After subtraction of the incoherent contribution the coherent SANS cross-section was obtained. The following figures show the corrected SANS cross-section.

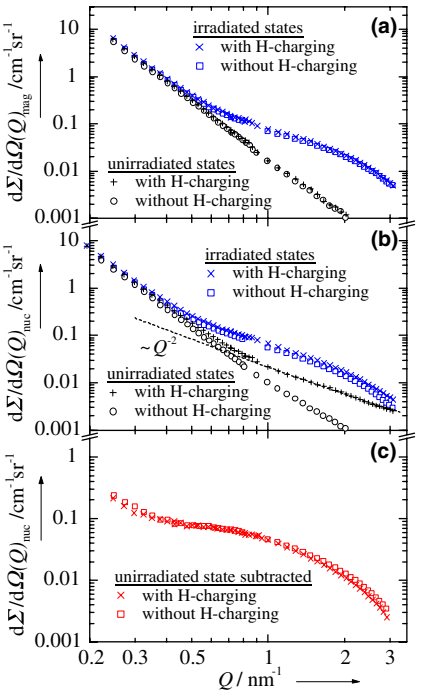

Fig. 1. SANS cross-section (a) magnetic and (b) nuclear for material JRQ in different conditions; (c) difference of the nuclear SANS cross-sections of irradiated and unirradiated conditions.

4. Results and discussion

Fig. 1 shows the magnetic and nuclear SANS cross-section for the JRQ material. For $Q > 0.5\,nm^{-1}$, the SANS cross-section of the irradiated state is clearly higher than for the unirradiated state. This proves the irradiation-induced production of nano-scaled microstructural defects. Hydrogen charging does not result in any noticeable changes of the magnetic SANS cross-section. However, the nuclear components are enhanced by hydrogen charging. This is, above all, evident for the unirradiated state, whereas the irradiated sample shows only a weak increase. The remarkable increase of the cross-section has a Q^{-2}-dependence as Fig. 1(b) shows. It could indicate an interfacial interaction between hydrogen and precipitates but exclude a hydrogen–dislocation interaction. In the last case a slope of −1 would be expected due to small-angle scattering of line-type defects.

The slight increase of the SANS cross-section after hydrogen charging disappears in the irradiated condition if the nuclear SANS cross-section of the unirradiated state is subtracted as depicted in Fig. 1(c). This permits the conclusion, that fine particles or microstructural heterogeneities which already exist in the unirradiated state, and not the radiation defects act as effective traps for hydrogen.

Similar results were obtained on the other materials. The SANS cross-section for the irradiated samples of JPA and KAB 7 are depicted in Figs. 2 and 3. Here, in contrast to JRQ, it was not the same sample measured in the uncharged and charged conditions. Nevertheless, the magnetic SANS cross-section curves for both conditions are almost identical. Whereas the nuclear SANS cross-section of the KAB-7-material is not changed by hydrogen charging as well, JPA shows a marked increase of the nuclear SANS cross-section compared with the uncharged sample for $Q < 0.5\,nm^{-1}$. This can be interpreted as a result of hydrogen trapping on precipitates having a radius >2 nm, e.g. carbides.

For samples of the KAB-8 material, the irradiation effect is lower but the hydrogen charging effect is again only evident in the unirradiated condition. This is shown in Fig. 4. The subtraction curves (Fig. 4(c)) are not completely identical for this material. It can be caused by material inhomogeneities. Obviously, the larger microstructural heterogeneities, which scatter into the lower Q value range, are especially effective as hydrogen traps. Such heterogeneities could be the small vanadium carbides with sizes of 8–20 nm which are typical for the vanadium alloyed 15Kh2MFA steel KAB-8 [30]. As

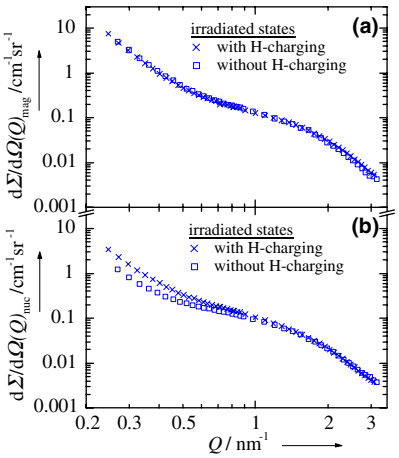

Fig. 2. SANS cross-section (a) magnetic, (b) nuclear for material JPA irradiated.

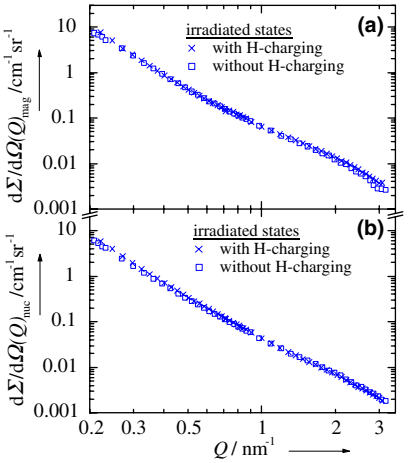

Fig. 3. SANS cross-section (a) magnetic, (b) nuclear for material KAB-7 irradiated.

known, small carbides with coherent or semi-coherent interfaces have been identified as especially effective hydrogen traps [34].

All materials considered so far have a high-copper content and, thus, the irradiation defects should be copper-rich precipitates or copper-enriched clusters according to the most dominant interpretation in the literature [35] and in correspondence with the A-ratio measured [30]. The binding energy between copper and hydrogen is low and, in a very simple approach, one can assume that the trap effectivity of such copper-enriched clusters is low as well.

In contrast to that, the weld metal R19 has a very low Cu content. This result is shown in Fig. 5. Unfortu-

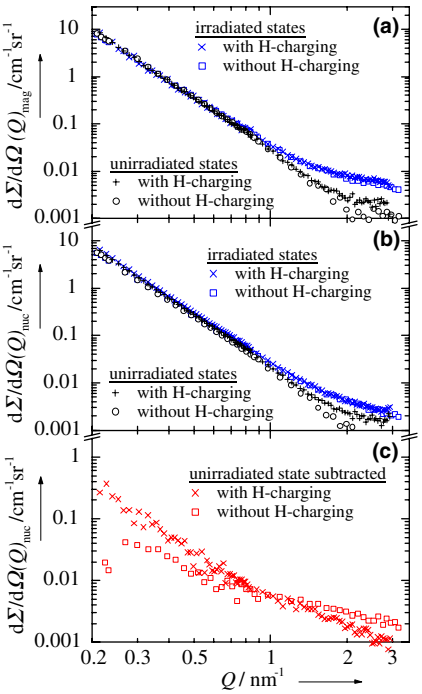

Fig. 4. SANS cross-section (a) magnetic and (b) nuclear for material KAB-8 in different conditions; (c) difference of the nuclear SANS cross-sections of irradiated and unirradiated conditions.

nately, the testing samples for the H-charged and uncharged states were not cut from the same Charpy specimen. So, there are larger differences in the microstructure, which even leads to differences in the magnetic SANS cross-section. Nevertheless, a higher nuclear scattering of H-charged specimens is only observed in the case of the unirradiated material but not for the irradiated material.

Obviously, hydrogen charging enhances the nuclear component of the small-angle scattering. Type, chemical composition and metallurgical treatment influence both the intensity and Q-dependence of the effect. However, an enrichment of hydrogen at the irradiation-induced microstructural defects cannot be proven for the steel types and the fluence range investigated. Therefore, under the chosen conditions, the results do not confirm the hypothesis of a direct interaction between radiation effect and hydrogen as suggested in [20] or [36]. On the other hand, the results do not exclude synergistic interactions between hydrogen and irradiation embrittlement mechanisms. Trapping of hydrogen at radiation defects is only a first simple approach of the potential interaction mechanisms. In addition hydrogen could affect the kinetics of the radiation defect evolution. Such processes can only be revealed by experiments with simultaneous irradiation and hydrogen charging.

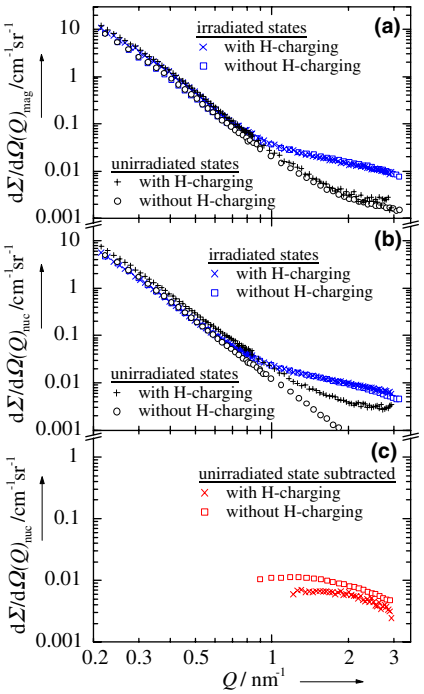

Fig. 5. SANS cross-section (a) magnetic, (b) nuclear for material R19 in different conditions, (c) difference of the nuclear SANS cross-sections of irradiated and unirradiated conditions.

5. Conclusion

A SANS study on samples from different unirradiated and irradiated RPV steels demonstrates that SANS has the capability to identify hydrogen trapping at small microstructural heterogeneities even if the bulk concentration of hydrogen is not higher than 1–2 ppm.

The hydrogen trapping effect depends on the type of materials. Preferentially, microstructural heterogeneities of the size of 8–20 nm are effective traps but also clearly smaller defects. However, the characteristic radiation defects in the size range of approx. 1 nm seem to be not effective as hydrogen traps.

Acknowledgments

The authors thank Mr P. Strunz from HMI Berlin for supporting the SANS measurements and their evaluation. The work was sponsored by the Bundesministerium für Wirtschaft und Arbeit under contract GRS 150 1267. The authors are grateful for the sponsorship.

References

[1] I.M. Bernstein, G.M. Pressouyre, in: R.A. Oriani, J.P. Hirth, M. Smidowski (Eds.), Hydrogen Degradation of Ferrous Alloys, Park Ridge, New Jersey, 1985, p. 641.
[2] C.R. Brinkmann, J.M. Beeston, The Effect of Hydrogen on the Ductile Properties of Irradiated Pressure Vessels, IN-1359, Rep., Idaho, Nuclear Cooperation, National Reactor Testing Station, 1972.
[3] H. Takaku, H. Kayano, S. Yajima, J. Nucl. Mater. 71 (1978) 292.
[4] H. Takaku, H. Kayano, J. Nucl. Mater. 78 (1978) 299.
[5] H. Takaku, H. Kayano, J. Nucl. Mater. 110 (1982) 286.
[6] M.C. Gupta, D.W. Höppner, W. Meyer, Nucl. Eng. Des. 36 (1976) 102.
[7] J. Koutsky, K. Splichal, Metall. Mater. 23 (1985) 352.
[8] J. Koutsky, K. Splichal, Int. J. Press. Vess. Piping 24 (1986) 13.
[9] N.N. Aleksandro, A.A. Nikolaev, E.P. Usatov, V.S. Fetisov, Fizikokhimicheskaja Mech. Mater. 13 (1977) 14.
[10] K. Splichal, M. Ruscak, J. Zdarek, Int. J. Press. Vess. Piping 55 (1993) 361.
[11] D. Anders, J. Föhl, Nucl. Eng. Des. 136 (1992) 265.
[12] M. Beghini, G. Benamati, L. Bertini, I. Ricapito, R. Valentini, J. Nucl. Mater. 288 (2001) 1.
[13] A. Kimura, H. Kayano, M. Narui, J. Nucl. Mater. 179–181 (1991) 737.
[14] P. Scott, J. Nucl. Mater. 211 (1994) 101.
[15] P.L. Andresen, in: R.H. Jones (Ed.), Stress corrosion cracking – material performance and evaluation, ASM, 1992, p. 181.
[16] H. Hänninen, Lecture on 20th Meeting of AMES Steering Committee, Paris, March 2000.
[17] M. Uhlemann, G. Müller, J. Böhmert, Hydrogen embrittlement of reactor pressure vessel steels, in: Proceedings of the 2nd International Conference EDEM, Bordeaux, 2003, H3-3-06.
[18] B. Pastina, J. Isabey, B. Hicked, J. Nucl. Mater. 264 (1999) 309.
[19] B. Tirbonod, Stress corrosion cracking: short description and review of models, Paul–Scherrer-Institut, PSI-Report TM-49-96-09, 1996.
[20] D. Pachur, The effect of hydrogen and oxygen on irradiation embrittlement of reactor pressure vessel steels, paper on the 18th International Symposium on Effects of Radiation on Materials, 22–25 June 1996, Hyannis, Massachusetts.
[21] D. Pachur, Nucl. Technol. 59 (1982) 463.
[22] L. Koester, H. Rauch, E. Seymann, Neutron scattering length: a survey of experimental data and methods, At. Data Nucl. Tabl. 49 (1991) 65.
[23] M. Maxelon, A. Pundt, W. Pyckhout-Hintzen, J. Barker, R. Kirchheim, Acta Mater. 49 (2001) 2625.
[24] M. Maxelon, A. Pundt, W. Pyckhout-Hintzen, R. Kirchheim, Scr. Mater. 44 (2001) 817.
[25] D.K. Ross, K. Stefanopoulos, M. Kemali, J. Alloys Compd. 293–295 (1999) 346.
[26] C.E. Buckley, H.K. Birnbaum, D. Bellmann, P. Staron, J. Alloys Compd. 293–295 (1999) 231.
[27] C.E. Buckley, H.K. Birnbaum, J.S. Lin, S. Spooner, D. Bellmann, P. Staron, T.J. Udovic, E. Hollar, J. Appl. Crystallogr. 34 (2001) 119.
[28] G. Kostorz, X-ray and neutron scattering, in: R.W. Cahn, P. Haasen (Eds.), Physical Metallurgy, vol. 2, North-Holland, Amsterdam, 1996, p. 1115, Chapter 12.
[29] O. Glatter, J. Appl. Crystallogr. 13 (1980) 7.
[30] J. Böhmert, A. Gokhman, M. Große, A. Ulbricht: Nachweis, Interpretation und Bewertung bestrahlungsbedingter

Gefügeänderungen in WWER-Reaktordruckbehäl-terstählen, Forschungszentrum Rossendorf, Wiss.-techn. Bericht FZR-381 (2003).
[31] U. Keiderling, A. Wiedemann, Physica B 213&214 (1995) 835.
[32] P. Strunz, J. Saroun, U. Keiderling, A. Wiedemann, R. Przenioslo, J. Appl. Crystallogr. 33 (2000) 829.
[33] M. Große, J. Böhmert, in: M.L. Hamilton, A.S. Kumar, S.T. Rosinski, M.L. Grossbeck (Eds.), Effects on Radiation on Materials: 19th International Symposium, ASTM-STP 1366, American Society for Testing and Materials, West Conshohocken, PA, 2000, p. 323.
[34] N. Paroathavarthini, S. Saroja, R.K. Dayal, H.S. Khatak, J. Nucl. Mater. 288 (2001) 187.
[35] G.R. Odette, G.E. Lucas, Radiat. Eff. Def. Solids 144 (1998) 189.
[36] T. Kato, K. Nakata, J. Kuniya, S. Oknuki, H. Takashi, J. Nucl. Mater. 155–157 (1988) 856.